Received: 1 March 2017 | Revised: 4 June 2017 | Accepted: 10 June 2017

DOI: 10.1111/cbdd.13063

RESEARCH ARTICLE

WILEY

# OM-LV20, a novel peptide from odorous frog skin, accelerates wound healing in vitro and in vivo

**Xiaojie Li**[1] | **Ying Wang**[2] | **Zhirong Zou**[3] | **Meifeng Yang**[3] | **Chunyun Wu**[3] | **Yunshan Su**[4] | **Jing Tang**[1] | **Xinwang Yang**[3]

[1]Department of Biochemistry and Molecular Biology, Faculty of Basic Medical Science, Kunming Medical University, Kunming, Yunnan, China

[2]Ethic Drug Screening & Pharmacology Center, Key Laboratory of Chemistry in Ethnic Medicine Resource, State Ethnic Affairs Commission & Ministry of Education, Yunnan MinZu University, Kunming, Yunnan, China

[3]Department of Anatomy and Histology & Embryology, Faculty of Basic Medical Science, Kunming Medical University, Kunming, Yunnan, China

[4]Department of Radiology, Second People's Hospital of Yunnan Province, Kunming, Yunnan, China

**Correspondence**
Xinwang Yang, Department of Anatomy and Histology & Embryology, Faculty of Basic Medical Science, Kunming Medical University, Kunming, Yunnan, China.
Email: yangxinwanghp@163.com
and
Jing Tang, Department of Biochemistry and Molecular Biology, Faculty of Basic Medical Science, Kunming Medical University, Kunming, Yunnan, China.
Email: gracett916@163.com

**Funding information**
Chinese National Natural Science Foundation, Grant/Award Number: 31660244, 31460571 and 31670776

The healing of chronic wounds remains a considerable challenge in clinical trials and imposes severe financial and physiological burdens on patients. Many works are being tried to find ideal clinical promoting wound healing biomaterials. Small bioactive peptides with low cost and easy production, store and transfer become excellent candidates. Here, we identified a novel peptide (named OM-LV20) from skin secretions of odorous frog *Odorrana margaretae*. The peptide had an amino acid sequence of "LVGKLLKGAVGDVCGLLPIC," contained an intramolecular disulfide bridge at the C-terminus, and was produced by post-translational processing of a 71-residue prepropeptide. Our results showed that OM-LV20 had no direct microbe-killing effects, hemolytic activity, or acute toxicity, but did exhibit weak antioxidant activity. OM-LV20 promoted wound healing against human keratinocytes (HaCaT) and human skin fibroblasts (HSF) in both time- and dose-dependent manners. In addition, it induced the proliferation of HaCaT but not HSF cells. Of note, OM-LV20 showed strong wound healing-promoting activity in a mice model of full-thickness skin wound. Our research indicates the cellular and animal level wound healing potential of OM-LV20, and thus provides a novel bioactive peptide template for the development of wound healing agents and medicine.

**KEYWORDS**
odorous frog, *Odorrana margaretae*, peptide, wound healing

## 1 | INTRODUCTION

Skin is the physical barrier between the inner body and outer surroundings and performs crucial physiological functions, such as perspiration and heat and pain sensation. Skin protects the inner organs and tissues from damage caused by physical, mechanical, and chemical factors, as well as pathogenic micro-organisms, which can induce skin rupture and infection.[1,2] Skin consists of two tissue layers: a keratinized stratified epidermis and an underlying thick layer of collagen-rich dermal connective tissue providing support and nourishment.[1] Following injury, skin must commence rapid repair,

Xiaojie Li and Ying Wang contributed equally to this work.

  

a complex and dynamic process that includes hemostasis, inflammation, cell proliferation, and tissue reconstruction.[3] The healing process of skin is comprehensive and time sensitive and can be interrupted by many factors, resulting in non-healing chronic wounds or unhealing skin ulcer. Many pathogens can take advantage of such situations and cause secondary infections, as well as water and electrolyte disturbance, infectious shock, multiple organ failure, and even death.[4,5] Thus, rapid and efficient wound healing is really crucial for human health and survival.

With the increase in chronic wounds due to aging populations and the growing prevalence of diabetes, uremia, and traffic accidents over the past several decades, wound healing continues to be a considerable challenge in clinical trials. In addition, wounds and their treatment impose a severe financial burden on human society. In the USA, for example, wound healing costs presently exceed US$30 billion per year.[6] Considering that no satisfactory healing methods and agents currently exist for secondary chronic wounds, the development of medicine and treatment to promote wound healing is crucial. Existing wound healing drugs can be classified into two main groups: small molecule compounds derived from plants and proteins typified by epidermal growth factors (EGFs). However, these drugs also possess unsatisfactory properties; for example, the former compounds are unstable with relatively low activity, and the latter proteins are expensive, require rigorous preservation conditions, and are liable to cause hyperplastic scars.[7] Therefore, the development of novel wound healing drugs that avoid or limit these disadvantages is critical.[8] Compared with small molecule compounds and growth factors, peptides possess high activity, stability, and specificity, and have aroused considerable global attention. Several peptide drugs, such as Copaxone, Exenatide, and Teriparatide Acetate, are considered the best choice for patients who are suffering from multiple sclerosis, type 2 diabetes mellitus, or osteoporosis and have achieved significant financial success. Active peptides are thus a very important element for drug discovery.[9,10]

Amphibian skins can secrete diverse bioactive peptides, including antimicrobial, antioxidant peptides, wound healing-promoting peptides, lectins, bradykinin, neuromedin, and neurotoxin.[11,12] Their structural novelty and functional diversity suggest they can be developed into a wide variety of novel drugs.[13] Research has shown that amphibian skins can heal rapidly without scarring,[14–16] and thus it is reasonable to assume that certain molecules found within these secretions undertake this crucial wound healing responsibility[17–19]; however, which molecules are involved remains unclear and, to date, only four wound healing peptides have been identified in amphibians.[20–23] Thus, knowledge on amphibian skin wound healing peptides is limited and requires further research.

Among amphibians, odorous frogs can secrete diverse bioactive peptides.[24] In the current research, a novel peptide, named OM-LV20, was identified from the skin secretions of *Odorrana margaretae*, and promoted potent wound healing activity in both cellular and animal models. Our results provide a novel template for the development of wound healing peptide candidates.

## 2 | MATERIALS AND METHODS

### 2.1 | Sample collection and animal care

Adult *O. margaretae* specimens ($n = 36$) were collected in the Guizhou Province of China and transferred to the laboratory safely. The frogs were housed together in a 50 cm × 65 cm container and provided with mealworms ad libitum. The frogs were acclimated for 2 days before the commencement of the experiments. The odorous frogs were placed in $H_2O$ containing 0.01% NaCl and were then stimulated by an alternating current (6 V) using an electronic massager for 6 s, with skin secretions collected by washing the frog bodies with 25 mM Tris–HCl buffer (pH 7.8). The collected solutions were centrifuged at 2880 *g* for 15 min at 4°C, and the supernatants were collected, lyophilized, and stored at −80°C until use.

All animal care and handling procedures were conducted in accordance with the requirements of the Ethics Committee of Kunming Medical University.

### 2.2 | Purification procedure

The purification procedure was performed as per previous research.[24] Briefly, the dissolved lyophilized skin secretion samples (500 μl, $OD_{280} = 70$) were applied to a Sephadex G-75 (1.5 × 31 cm, superfine, GE Healthcare, Sweden) gel filtration column pre-equilibrated with 25 mM Tris-HCl buffer (pH 7.8) containing 0.1 M NaCl, with elution performed using the same buffer at a flow rate of 0.1 ml/min. Fractions were collected using an automatic fraction collector (BSA-30A, HuXi Company, Shanghai, China) every 10 min and monitored at 280 nm. Fractions were desalted by a reverse phase HPLC (RP-HPLC) on a C4 column (4.6 × 250 mm, Elite, China) then lyophilized, redissolved in 500 μl DMEM/F12 medium (BI, Israel), and their wound healing activities on HaCaT cells were tested. Fractions with cellular-level wound healing activity were merged together and then applied to a C18 RP-HPLC column (Hypersil BDS C18, 4.0 × 300 mm, Elite, China) pre-equilibrated with 0.1% (v/v) trifluoroacetic acid (TFA) in water. Elution was achieved by a linear gradient (0%–70% ACN in 70 min, as shown in Figure 1b,c) of 0.1% (v/v) TFA in acetonitrile (ACN) at a flow rate of 1 ml/min and monitored at 215 nm. Peaks with cellular-level wound healing activity were collected and lyophilized for a

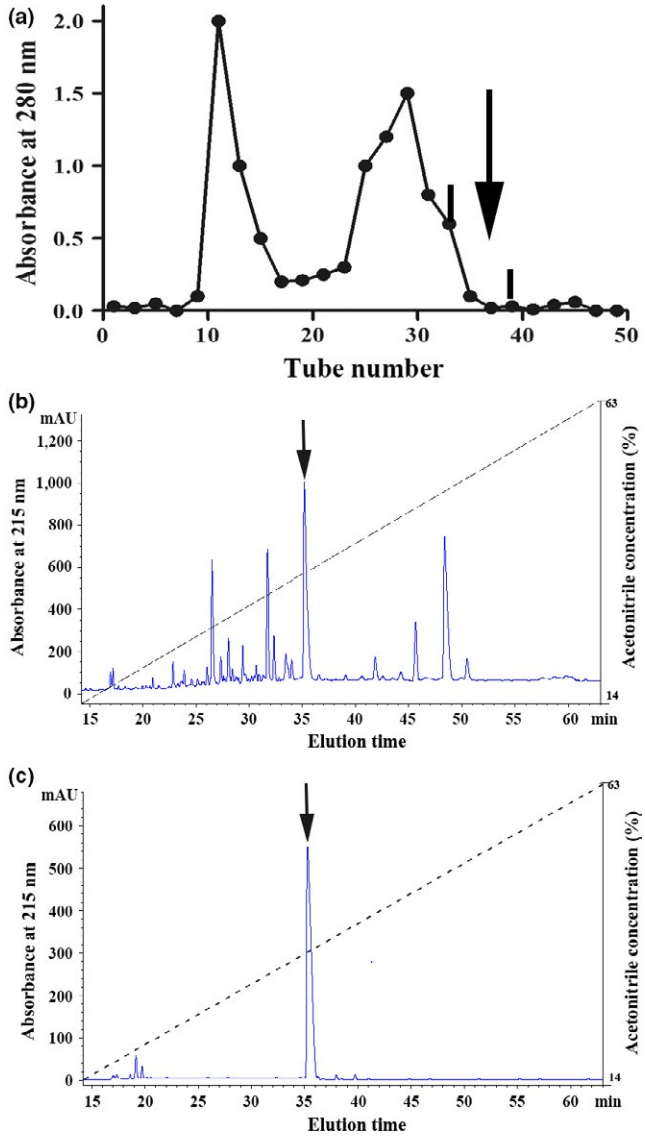


**FIGURE 1** Peptide purification procedures from skin secretions of *O. margaretae*. Skin secretions of *O. margaretae* were separated by a Sephadex G-75 column, and samples exhibiting wound healing activity was indicated by an arrow (a) and further purified by a round of RP-HPLC, the sample with wound healing activity was indicated by an arrow (b) and then further purified by another round of RP-HPLC by identical procedure with the first round of RP-HPLC, finally, a peptide with wound healing activity was obtained (indicated by an arrow in c) and awaiting further research

second HPLC purification procedure using the same conditions as above. Peptides were tracked by wound healing activity on HaCaT cells as described in detail in Section 2.10.

## 2.3 | Determination of peptide primary structure

The average molecular mass and the purity of native OM-LV20 were determined using an AXIMA-CFRTM plus MALDI-TOF mass spectrometer (Shimadzu/Kratos, Manchester, UK) in linear mode with α-cyano-4-hydroxycinnamic acid as the matrix. All procedures were carried out per the manufacturer's standard protocols, and data were analyzed using the provided software package. To obtain the complete amino acid sequence, the peptide was directly subjected to Edman degradation on a PPSQ-31A protein sequencer (Shimadzu, Japan) according to the manufacturer's standard GFD protocols, and the recognition of cysteine residues was conducted according to the standard protocols provided by the manufacturer.

## 2.4 | Cloning of cDNA encoding OM-LV20

An *O. margaretae* skin cDNA library was successfully constructed in our previous research,[24] with the cDNA encoding mature peptide screened from this library. Briefly, the 5′ PCR primer (5′-CCAAA(G/C)ATGTTCACC(T/A) TGAAGAAA-3′) and 3′ PCR primer (5′-ATTCTAGA GGCCGAGGCGGCCGACATG-3′) were commercially synthesized and provided by the BGI Company (China). PrimeSTAR® HS DNA Polymerase (TaKaRa Biotechnology Co., Ltd., Dalian, China) was selected for polymerase chain reaction (PCR) under the following conditions: 2 min at 94°C and then 25 cycles of 10 s at 92°C, 30 s at 50°C, and 40 s at 72°C. The PCR products were recovered using a DNA Gel Extraction Kit (Bioteke, China) and ligated into a pMD19-T Vector (TaKaRa Biotechnology Co., Ltd., Dalian, China). The PCR products were finally cloned into *Escherichia coli* DH5α, and independent clones were chosen to carry out DNA sequencing on an Applied Biosystems DNA sequencer (ABI 3730XL, Foster City, CA, USA).

## 2.5 | Peptide synthesis

The mature OM-LV20 peptide (LVGKLLKGAVGDVC GLLPIC) was commercially synthesized by GL Biochem Ltd. (Shanghai, China) and Wuhan Bioyeargene Biotechnology Co., Ltd. (Wuhan, China). The synthesized OM-LV20 was analyzed by Mass spectrometer, co-eluted with the natural OM-LV20 and confirmed to be identical with the native OM-LV20. The biological activities of the synthesized OM-LV20 were then tested.

## 2.6 | Antimicrobial activity assay

Highly sensitive radial diffusion was used according to our previous research.[25] Briefly, Gram-positive bacterial strain *Staphylococcus aureus* (ATCC 25923), Gram-negative bacterial strains *E. coli* (ATCC 25922) and *Bacillus pyocyaneus* (CMCCB 10104), and fungal strain *Candida albicans* (ATCC 2002) were obtained from the Kunming Medical University. The microbes were grown in *Luria Bertani* (LB) broth to an $OD_{600}$ of 0.8. A 10 μl aliquot of the bacteria was then taken and added to 10 ml of fresh LB broth with 1%

Type I agar (Sigma-Aldrich, St Louis, MO, USA) and poured over a 90 mm Petri dish. After the agar hardened, a small hole was made, and a 7 µl aliquot of OM-LV20 (1 mM) was added to the hole, which was then completely dried and incubated over night at 37°C. If an examined sample contained antimicrobial activity, a clear zone formed on the surface of the agar representing inhibition of bacterial growth. Minimal inhibitory concentration (MIC) was determined in liquid LB medium at pH 7.0 by conventional serial dilution in 96-well microtiter plates. The MIC value, at which no bacterial growth occurred, was recorded by measuring the absorbance at 600 nm after incubating at 37°C for 16–18 hr. In these experiments, ampicillin (1 mg/ml) and Nigrocin-OA1 (an antimicrobial peptide identified in our previous report[24]) were used as positive controls.

## 2.7 | Antioxidant activity assay

A 2, 2′-azino-bis (3-ethylbenzothiazoline-6-sulfonic acid) (ABTS) scavenging test was performed as described previously, with some modification.[12] Briefly, a stock solution of ABTS radical (Sigma-Aldrich) was prepared by incubating 2.8 mM potassium persulfate (Sigma-Aldrich) with 7 mM ABTS in water for at least 6 hr in the dark, after which it was used immediately. The stock solution was diluted 50-fold with deionized water. Samples dissolved in water were added, with the same volume of solvent was used as the negative control. Vitamin C dissolved in $H_2O$ was used as the positive control. The reaction was kept from light for 30 min. The decrease in absorbance at 415 nm indicated the antioxidant activity of the samples. The rate of free radical scavenging (%) was calculated by $(A_{blank} - A_{sample}) \times 100/A_{blank}$.[12]

A 2, 2-diphenyl-1-picrylhydrazyl (DPPH) scavenging test was also performed as described previously,[26] with some modification. Briefly, the assay mixture contained 190 µl of $5 \times 10^{-5}$ M DPPH radical (Sigma-Aldrich) dissolved in methanol. The sample solution (10 µl) was then incubated in a sealed 1.5-ml microcentrifuge tube for 30 min at room temperature, and absorbance was read against a blank at 517 nm. The DPPH scavenging activity (%) was calculated by $(A_{blank} - A_{sample}) \times 100/A_{blank}$.

Scavenging of nitric oxide (NO) was determined by incubating 5 mM sodium nitroprusside dihydrate (SNP; Sigma-Aldrich) in PBS with different concentrations of samples at 25°C. After 120 min, 0.5 ml of incubation solution was withdrawn and mixed with 0.5 ml of Griess reagent. Absorbance was measured at 550 nm. The amount of NO was calculated from a standard curve constructed using sodium nitrite.

## 2.8 | Hemolytic activity assay

Hemolytic activity was tested as described previously.[25] In short, human erythrocytes were thrice washed with Dulbecco's phosphate-buffered saline. Cells were incubated with various doses of the OM-LV20 peptide at 37°C in a water bath for 30 min. After centrifugation at 4000 *g* for 4 min at room temperature, absorbance of the supernatant was measured at 540 nm. Incubation with 1% Triton X-100 was carried out to determine maximum hemolysis.

## 2.9 | Acute toxicity assay

Acute toxicity was determined in two phases as described previously.[27] Lethal range acute toxicity of the OM-LV20 test samples was determined at concentrations of 5, 10, 50, and 100 mg/kg by intraperitoneal (i.p.) injection in mice. Mice were observed for 24 hr, and the mortalities, toxic effects, and changes in behavioral patterns were recorded.

## 2.10 | Cellular wound healing activity assay

Cellular wound healing was determined according to earlier research,[20] with some modification. In short, immortalized HaCaT cells and human skin fibroblasts (HSFs) were cultured in DMEM/F12 medium (BI, Israel) with 10% fetal bovine serum (FBS, BI, Israel), 100 units/ml of streptomycin, and 100 units/ml of penicillin in a humidified atmosphere of 5% $CO_2$ at 37°C. Cell monolayer formation was achieved by culturing the HaCaT and HSF ($2.5 \times 10^5$ cells/well) cells in 24-well plates for 12–24 hr. Serum starvation for 24 hr was performed for increasing the peptide sensitivity. The cell monolayers were then wounded using a yellow 200 µl pipette tip (Axygen, USA), and twice washed with PBS to remove any detached cells. Subsequently, DMEM/F12 medium—serum-free (500 µl)—containing various concentrations of OM-LV20 (0.5, 1, 2.5, 5, 10 nM) was respectively added to each well with or without mitomycin C (10 µg/ml, Sigma-Aldrich). Images of the wound healing monolayers were acquired using a Primovert microscope (Zeiss, Germany) at time intervals of 0, 12, and 24 hr. Cell migration activity was expressed as the percentage of the gap relative to the total area of the cell-free region immediately after the scratch, named the repair rate of scarification, using IMAGE J software (National Institutes of Health, Bethesda, MD, USA). For each plate, six randomly selected images were acquired. All experiments were independently carried out in triplicate.

## 2.11 | HaCaT and HSF cell proliferation assays

Cells were cultured in DMEM/F12 medium with 10% FBS, 100 units/ml of streptomycin, and 100 units/ml of penicillin in a humidified atmosphere of 5% $CO_2$ at 37°C. The cells (5,000 HaCaT cells and 10,000 HSF cells per well, 100 µl, respectively) were then plated in 96-well plates

and incubated for 4 hr to allow the cells to adhere to the well walls. Subsequently, 20 μl of OM-LV20 dissolved in DMEM (serum-free) at various concentrations (0.5, 1, 2.5, 5, 10 nM) was added to each well, followed by a further 24 hr of incubation. The same volume of DMEM (serum-free) was used as a blank control. After incubation, the CellTiter 96® AQueous One Solution Assay (Promega, Madison, WI, USA) was used in accordance with the manufacturer's instructions to test the effect of OM-LV20 on HSF and HaCaT cell proliferation.[24]

### 2.12 | Animal wound healing assay

We obtained 20 adult male mice (22–25 g) from the Experimental Animal Center of Kunming Medical University. The mice were kept individually in cages at room temperature, and provided with free access to water and laboratory chow. The animals were given 3 days to acclimate to the conditions before the commencement of the experiments. Full-thickness skin wounds were then surgically applied. The animals were anesthetized with intraperitoneal injection of 100 ml solution containing 1% pentobarbital sodium (0.1 ml/20 g body weight). The dorsal hair of the mouse was shaved and disinfected with 70% ethanol swab to prepare the back skin for generation of a standardized full-thickness cutaneous wound. Two 8 × 8 mm full-thickness excisional wounds were created on the back of each mouse. At the end of the surgical procedure, cages were placed near to a heating apparatus until mice fully recovered from anesthesia.

Mice bearing full-thickness wound were randomly divided into two groups of animals each. The left-sided wounds of the first group were treated with 20 μl (20 nM) of OM-LV20, with the same volume of saline used on the right-sided wounds; for the second group, the left-sided wounds were treated with 20 μl (20 nM) of OM-LV20, with the same volume of epidermal growth factor (EGF, 20 nM; Sigma-Aldrich) used for the right-sided wounds. All wounds on all mice were treated twice daily. The wounds were photted at time intervals of 3 days.[21]

### 2.13 | Wound healing rate measurement

The closure of the mouse wounds was recorded with a D3000 digital camera (Nikon, Japan). Wound areas (percentage of residual wound area to original wound area) were estimated from the photographs using IMAGE J software (NIH, USA), in which the edges of the wounds were traced, and the pixel areas were calculated. Mean values of successive tracings were computed as percentages of closure from the initial wound based on triplicate images using the following equation: Residual Wound Area (%) = [R(2, 9)/R(0)] × 100, where R(0) and R(2, 9) denote the remaining wound area at the same day of operation and postoperative days 2, 9, respectively. Wound healing curves were constructed by GRAPHPAD PRISM software (v. 5).

## 3 | RESULTS

### 3.1 | Peptide purification

Skin secretions of odorous frog *O. margaretae* were divided into two main peaks by gel filtration. The fraction samples was collected every 10 min from gel filtration and then tested for their wound healing activity on HaCaT cells. Samples that showed obvious activity (indicated by an arrow, Figure 1a) were merged further purified by HPLC. As shown in Figure 1b, more than 20 peaks were obtained, with one showing the intended activity. This peak was further purified by HPLC, and finally, one peak with an ideal shape and similar elution time (about 35.1 min) with that of the former HPLC procedure was obtained (Figure 1c). This sample was found to promote HaCaT cell wound healing (data not shown), and its primary structure was therefore determined.

### 3.2 | Primary structure of OM-LV20

The sample purified by the second RP-HPLC procedure (indicated by an arrow in Figure 1c) was analyzed by MS spectrometry, with its observed molecular mass determined to be 1966.39 Da (Figure 2b). Together with the chromatographic results from the second RP-HPLC procedure (Figure 1c), we assumed this sample possessed an ideal purity of >95% and was mainly composed of a peptide with a molecular mass of 1966.39 Da. Next, we determined the amino acid sequence of this peptide using an Edman sequencer, which revealed that the amino acid sequence from the N-terminus to C-terminus was "LVGKLLKGAVGDVCGLLPIC" (Figure 2a). To confirm this sequence, we successfully screened the cDNA encoding this peptide from a skin cDNA library, and the deduced sequence was well-matched with the Edman determined sequence. As shown in Figure 2a, the OM-LV20 peptide (OM: species name abbreviation, LV: two initial amino acids, 20: peptide length) was produced by post-translational processing of a 71-residue prepropeptide. The theoretical molecular mass (TMM), as calculated at http://web.expasy.org/compute_pi/, was 1968.49 Da; however, the observed molecular mass (OMM) was 1966.39 Da (Figure 2b), a difference of 2 Da. It should be noted that there were two cysteine residues located at the 14th and 20th positions of this peptide, and the 2 Da difference between the TMM and OMM values indicated the presence of an intramolecular disulfide bridge. We analyzed reduced native OM-LV20 with dithiothreitol (DTT) to open the assumed disulfide bridge. Results revealed that the OMM value was 1968.20 Da (Figure 2c), which

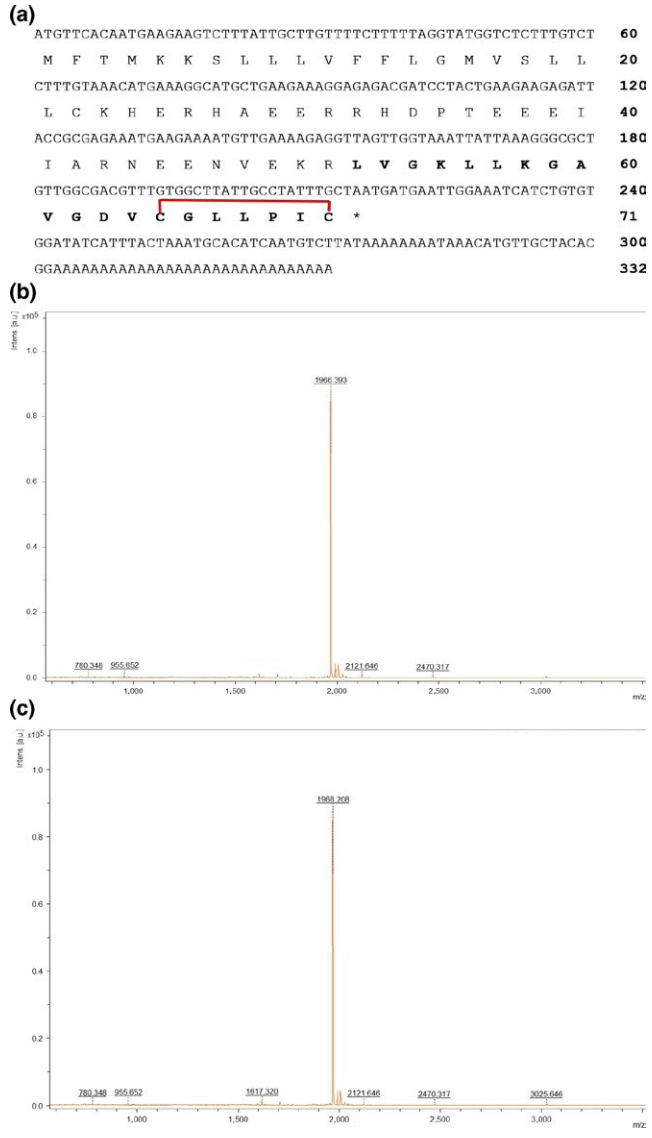


**FIGURE 2** Primary structure of OM-LV20. (a) Sequence of OM-LV20. The complete sequence of mature OM-LV20 was "LVGKLLKGAVGDVCGLLPIC," which was 20 amino acid residues-in-length (shown in bold) and produced by post-translational processing of a 71-residue prepropeptide. OM-LV20 contained an intramolecular disulfide bridge located at the C-terminus (indicated by red lines). (b) Observed molecular mass of native OM-LV20 and purity of peak, indicated by an arrow in Figure 1c. (c) Observed molecular mass of reduced OM-LV20

well-matched the TMM value. These findings indicated the existence of an intramolecular disulfide bridge located at the C-terminus of OM-LV20.

## 3.3 | OM-LV20 showed no direct antimicrobial activity, but did show weak antioxidant activity

At the maximum concentration of 1 mM, OM-LV20 showed no direct killing effect on Gram-positive bacterial strain *S. aureus*, Gram-negative bacterial strains *E. coli* and *B. pyocyaneus*, or fungal strain *C. albicans*. We also tested the antioxidant activity of OM-LV20. At the same concentration as above, OM-LV20 showed no scavenging activity against free radicals $ABTS^+$ or DPPH, but did scavenge 40.07 ± 5.8% (mean ± *SD*, $n = 3$) of NO.

## 3.4 | OM-LV20 showed no hemolytic activity against human blood cells or acute toxicity against mice

At a concentration of 1 mM, OM-LV20 showed no hemolytic activity. In regard to acute toxicity, no lethal effects were observed after a single i.p. injection of OM-LV20 at doses of 5, 10, 50, and 100 mg/kg after 24 hr (data not shown).

## 3.5 | OM-LV20 showed wound healing activity on HaCaT cells

During the healing of cutaneous wound, keratinocytes migration is very important. Pioneer keratinocytes, which early migrate to wound area and form neo-epithelial tongue to cover the wound incision, consequently, in favor of proper and timely wound reparation. An in vitro cells scratch assay was performed to investigate the effect of OM-LV20 on keratinocytes migration. Keratinocytes migration rate was based on the efficiency of monolayer cells invading the wound region with OM-LV20 treatment for 0–24 hr. Different gradient concentrations ranging from 0.5, 1, 2.5, 5, and 10 nM of OM-LV20 was employed to investigate its promoting HaCat cells migration activity. As shown in Figure 3a, after the application of the scratch wound, HaCaT cells showed a background healing rate of about 50% and 70% at 12 and 24 hr, respectively. Following treatment with OM-LV20 (10 nM), the healing rate significantly accelerated to about 80% and 95% at 12 and 24 hr, respectively. As shown in Figure 3c, OM-LV20 significantly promoted wound repair in both time- and dose-dependent manners. At concentrations ranging from 2.5 to 10 nM, OM-LV20 showed obvious HaCaT cell wound healing activity, with healing rates of more than 80% at 24 hr following the infliction of the wound. Compared with concentrations of OM-LV20, ranging from 0.5 to 1 nM, OM-LV20 showed strong dose-dependent activity at concentrations from 2.5 to 10 nM. Considering that cell proliferation and migration contribute to cellular wound healing, we inhibited the proliferation of HaCaT cells with mitomycin C, with the background healing rate was found to be lower than that of cells without mitomycin C (Figure 3a versus Figure 3b, Figure 3c versus Figure 3d). However, when treated with 10 nM OM-LV20, the healing rate of the HaCaT cells significantly increased to 68% at 12 hr and 90% at 24 hr (Figure 3b,d), and at concentrations ranging from 2.5 to 10 nM, OM-LV20 showed both dose- and time-dependent

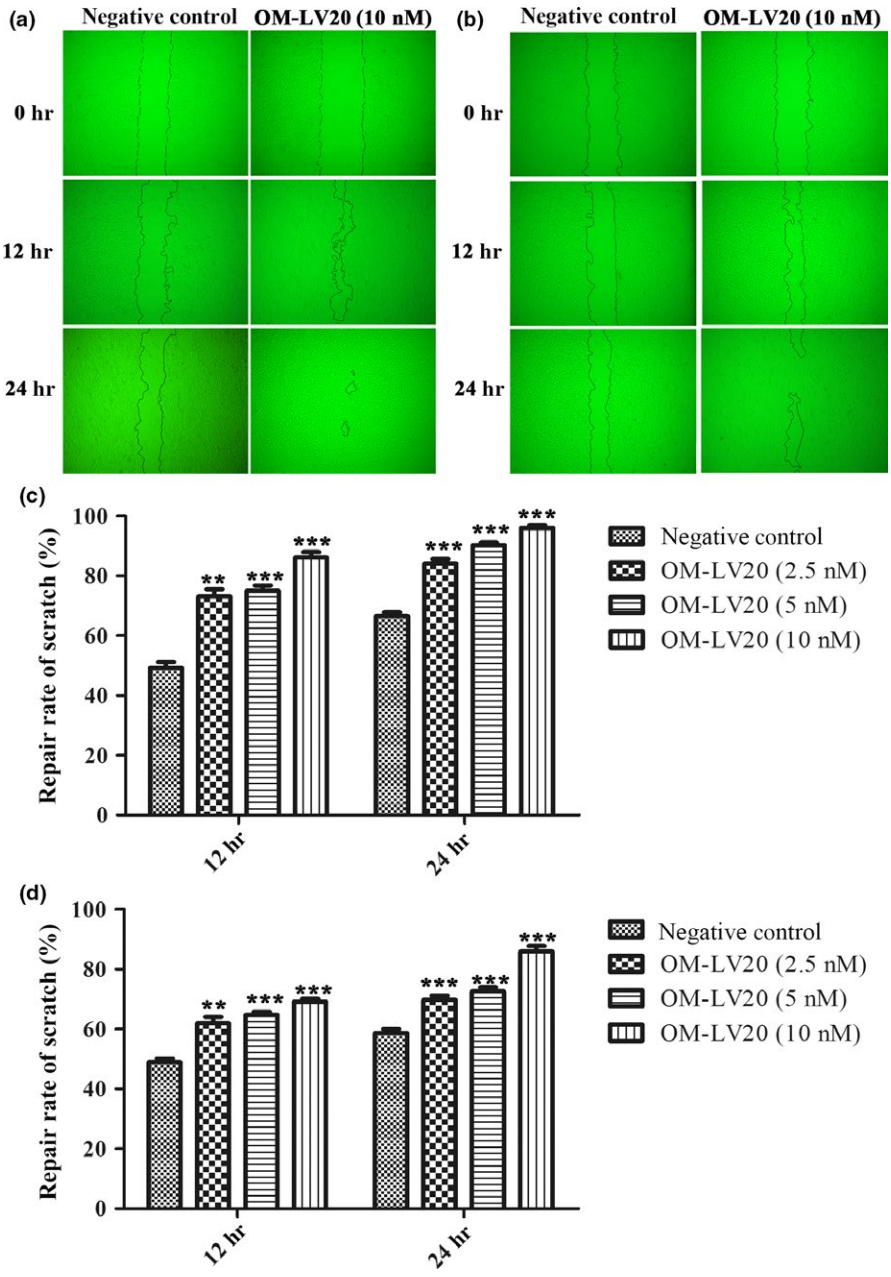


**FIGURE 3** Effect of OM-LV20 on the repair rate of HaCaT cell wounds. (a) OM-LV20 (10 nM) demonstrated significant HaCaT cell wound healing activity. (b) OM-LV20 (10 nM) demonstrated HaCaT cell wound healing activity when proliferation was inhibited by mitomycin C. (c) OM-LV20 demonstrated time- and dose-dependent HaCaT cell wound healing activity. (d) OM-LV20 demonstrated time- and dose-dependent HaCaT cell wound healing activity when proliferation was inhibited by mitomycin C. Data are means ± *SEM* of six independent experiments. $*p < .05$, $**p < .01$, and $***p < .0001$ indicate significantly different from the control (Student's *t* tests)

wound healing activity. In conclusion, regardless of whether the proliferation of HaCaT cells was inhibited or not, OM-LV20 showed both time- and dose-dependent wound healing activity on HaCaT cell wounds (scratches).

## 3.6 | OM-LV20 showed wound healing activity on HSF cells

Except for keratinocytes, fibroblasts migration also exerts predominant role during wound healing. Fibroblasts migration rate was based on the efficiency of monolayer cells invading the wound region with OM-LV20 treatment for 0–24 hr. The same as the HaCat cells wound healing activity test, gradient concentrations ranging from 0.5, 1, 2.5, 5, and 10 nM of OM-LV20 were employed to investigate its promoting HSF cells migration activity. OM-LV20 showed obvious time-dependent wound healing on HSF cells at the concentration of 2.5 nM (Figure 4a,c). For HSF cells, background healing rates of about 50% and 75% were detected 12 and 24 hr, respectively, after the infliction of the scratch wound (Figure 4c). However, when incubated with OM-LV20 at a concentration of 500 pM, the wound repair rate increased to almost 75% and 85%, respectively; moreover, this ability increased with the increase in concentration (ranging from 0.5 to 2.5 nM). For HSF cells, the obvious dose-dependent activity of OM-LV20 was not shown at concentrations from 5 and 10 nM. When the proliferation of HSF cells was inhibited by mitomycin C, the background healing rate partially decreased (Figure 4b,c), but OM-LV20 still induced healing in a time- and dose-dependent manner (Figure 4c).

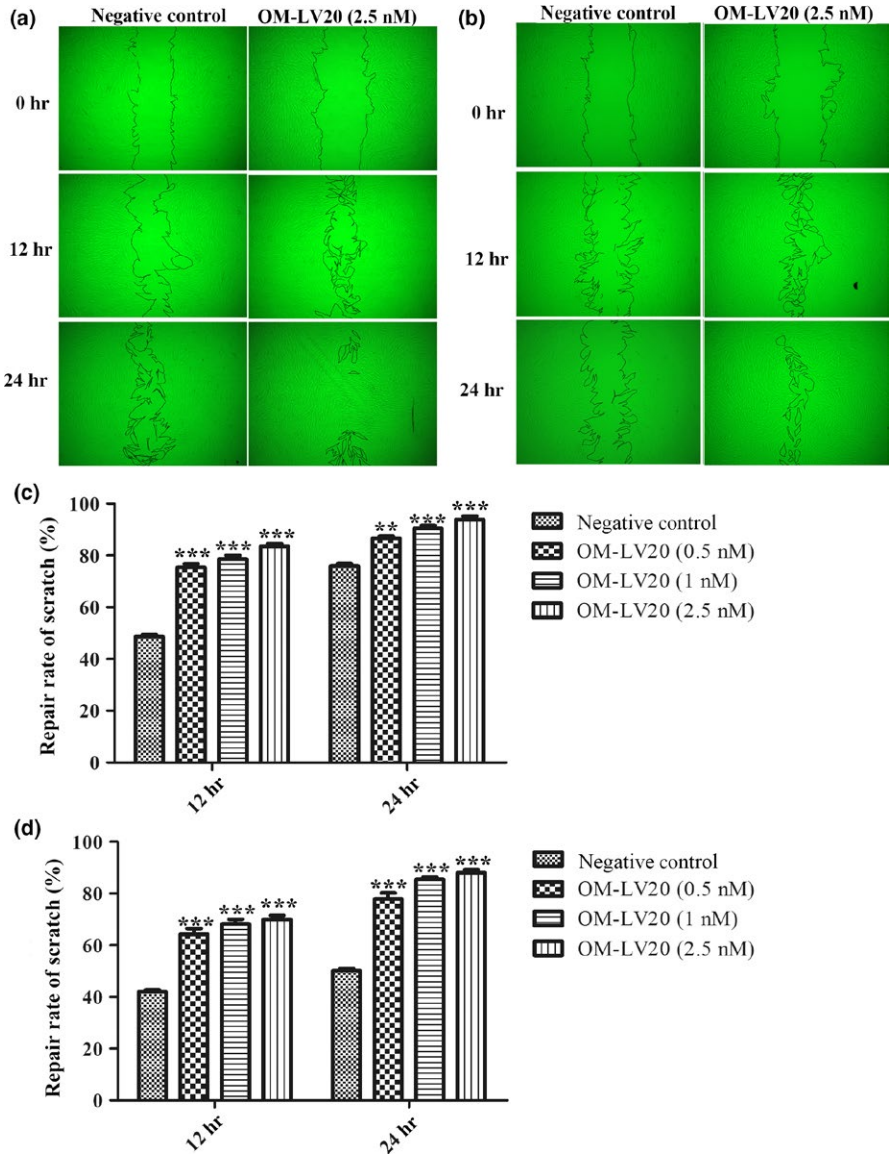


**FIGURE 4** Effect of OM-LV20 on the repair rate of HSF cell wounds (scratches). (a) OM-LV20 (2.5 nM) demonstrated significant HSF cell wound healing activity. (b) OM-LV20 (2.5 nM) demonstrated HSF cell wound healing activity when proliferation was inhibited by mitomycin C. (c) OM-LV20 demonstrated time- and dose-dependent HSF cell wound healing activity. (d) OM-LV20 demonstrated time- and dose-dependent HSF cell wound healing activity when proliferation was inhibited by mitomycin C. Data are means ± *SEM* of six independent experiments. ***$p < .0001$ indicates significantly different from the control (Student's *t* tests)

## 3.7 | OM-LV20 induced proliferation of HaCaT but not HSF cells

Keratinocytes and fibroblasts are important cells that dominantly take part in proliferation phase of wound healing. An in vitro cells proliferation assay was performed to investigate effects of OM-LV20 on cells proliferation. As illustrated in Figure 5a, OM-LV20 promoted HaCaT keratinocytes proliferation in a concentration-dependent manner. The wound healing potency of OM-LV20 decreased when the proliferation of HaCaT cells was inhibited by mitomycin C. This indicated that OM-LV20 affected the proliferation of HaCaT cells, which partially contributed to the wound healing potency of OM-LV20. As shown in Figure 5a, at concentrations

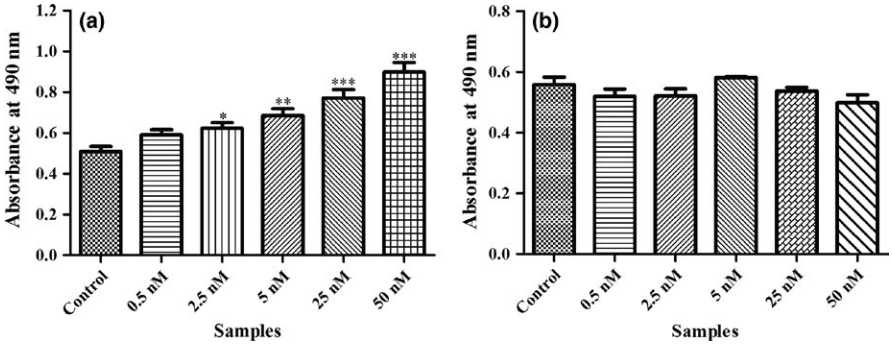


**FIGURE 5** Effects of OM-LV20 on the proliferation of HaCaT and HSF cells. (a) At concentrations of 2.5–50 nM, OM-LV20 showed proliferative effects on HaCaT cells. (b) At the same concentrations, OM-LV20 showed no effect on the proliferation of HSF cells. "Control" meant Negative control, *$p < .05$, **$p < .01$, and ***$p < .0001$ indicate significantly different from the control (Student's *t* tests)

of 2.5–50 nM, OM-LV20 showed a dose-dependent proliferative effect on HaCaT cells. At the same concentrations, however, OM-LV20 showed no obvious effects on HSF cell proliferation.

### 3.8 | OM-LV20 accelerated the healing of full-thickness wounds in mice

As OM-LV20 showed considerable cellular wound healing activity, it would be expected that OM-LV20 might accelerate wound reparation in vivo. A full-thickness skin wound healing model was used to assess the effects of OM-LV20 topical application on wound healing. Following the infliction of full-thickness skin wounds on mice, OM-LV20 (20 nM, 20 μl), EGF (positive control, 20 nM, 20 μl), or vehicle (saline, as negative control) was topically painted to the wounds twice daily. Images of the wounds were acquired on the same day of operation and postoperative day 4, 7, and 10, respectively. Compared with that of the control, the residual wound areas in the OM-LV20-treated mice on postinjury days 4, 7, and 10 were significantly decreased. Furthermore, 20 nM OM-LV20 showed similar healing activity as that of 20 nM EGF. Of note, mice exhibited no adverse effects on body weight, general health, or behavior after topical OM-LV20 treatment (data not shown). At concentrations of OM-LV20, from 0.5, 1, 2.5, 5, and 10 nM, the obvious promoting wound healing activity was not found on mice (data not shown), which may be interpreted by the difference response to cells in vitro and animals in vivo.

## 4 | DISCUSSION

Amphibian skin secretions are rich in bioactive peptides, with antimicrobial peptides, antioxidant peptides, lectins, and protease inhibitors formerly identified and characterized.[28,29] Amphibian skin secretions also promote obvious wound healing; to date, however, only four related bioactive peptides have been identified.[20–23] Odorous frog skins secrete diverse bioactive peptides, thus providing the potential for the discovery of new bioactive compounds.[24,30–32] This research aimed to identify novel wound healing peptides from odorous frog skin secretions.

Considering that many bioactive peptides show direct killing effects on normal cells at high concentrations,[11,33,34] we tested the cellular wound healing activities of the elutions collected from gel filtration chromatography individually with different low concentrations of OM-LV20. As shown in Figure 1a, samples that showed activity were combined and further purified by two RP-HPLC procedures (Figure 1b,c). Finally, a peptide with cellular-level wound healing activity was purified from the skin secretions of odorous frog *O. margaretae*. The complete peptide sequence was "LVGKLLKGAVGDVCGLLPIC," which was confirmed by Edman sequencing and cDNA cloning (Figure 2a). We performed Blastp searching in the NCBI database and found no peptide with a similar sequence, and thus, this peptide was considered novel and named OM-LV20. The cDNA cloning results indicated that OM-LV20 was produced by post-translational processing of a 71-residue prepropeptide (Figure 2a), which shared a highly conserved motif with other bioactive peptides from amphibian skins, and was divided into an N-terminal hydrophobic signal peptide, an acidic segment, and mature peptides at the C-terminal. The most common typical enzyme cleavage sites are composed of "Lys-Arg".[24,32] The 2 Da difference in the TMM (1968.49 Da) and OMW (1966.39 Da) indicated the existence of an intramolecular disulfide bridge located at the C-terminus,[35] which was confirmed by the OMM (1968.20 Da) of reduced native OM-LV20 (Figure 2b,c).

Most peptides from amphibian skins contain an intramolecular disulfide bridge located at the C-terminus, commonly referred to as the "Rana box," and show antimicrobial activities or toxic and cytolytic effects on normal cells.[11,24,33,34] Fortunately, even at high concentrations of 1 mM, OM-LV20 showed no hemolytic activity on human red blood cells and no acute toxic effects on animals. Because the overall structure of OM-LV20 is similar to that of other known amphibian skin bioactive peptides, a series of tests were performed. OM-LV20 showed no direct killing effect on Gram-positive bacterial strain *S. aureus*, Gram-negative bacterial strains *E. coli* and *B. pyocyaneus*, or fungal strain *C. albicans*. We also tested its antioxidant effects at the same concentration, and found that OM-LV20 showed no scavenging activities against free radicals $ABTS^+$ or DPPH, but did demonstrate weak activities on NO.

Keratinocytes and fibroblasts are important repairing cells that dominantly take part in proliferation phase of wound healing. In this research, gradient concentrations of OM-LV20, from 0.5, 1, 2.5, 5, and 10 nM, were respectively employed to detect the cellular-level wound healing activity. HaCat and HSF required different minimum concentrations (2.5 and 0.5 nM, respectively) to accelerate the healing rate. The dose-dependent wound healing-promoting activities of OM-LV20 on HaCat with concentrations ranging from 2.5 to 10 nM are shown in Figure 3. The effects of OM-LV20 at the concentrations of 5 and 10 nM showed no significant difference with that of 2.5 nM (Data not shown), which implied that only OM-LV20 of 2.5 nM achieved the maximum accelerative effect in this HSF assay. As correspondence, for HSF, data from three concentrations (0.5–2.5 nM) of OM-LV20 were observed the stronger dose-dependent activity of OM-LV20 (Figure 4), compared with concentrations from 5 and 10 nM. The possible reasons may be different migration

mechanism involved in different cells. For HaCat and HSF, different effective concentration may result in different integrin expression, which lead to HaCat cells or HSFs exert distinct migration activity on different peptide concentrations. Compared with the four related bioactive peptides,[20–23] OM-LV20 exerted more potential effects on wound repairing of HaCat and HSF cells, even with lower concentration. Many mechanisms play crucial roles in wound healing, including cell proliferation, cell migration, inflammation-related factors, and angiogenesis.[3] OM-LV20 exhibited proliferative effects on HaCaT cells (Figure 5a); however, when cells were treated with mitomycin C to inhibit cell proliferation, OM-LV20 still showed cellular wound healing activity (Figure 3b,d), although activity was decreased (Figure 3c,d). These results indicate that OM-LV20-induced wound healing of HaCaT cells was related, but not limited to cell proliferation, which might be correlated with its promotion effects on proliferation, migration, and adhesion of keratinocytes. In addition, OM-LV20 did not induce the proliferation of HSF cells (Figure 5b), but did accelerate wound repair (Figure 4b,d), implying that OM-LV20 induced HSF cell wound healing via cell migration, cell adhesion, or fibroblasts to myofibroblasts transition, rather than by proliferative effects. In conclusion, the mechanisms of OM-LV20 underlying cellular wound healing activity are complicated and await further research. Promisingly, OM-LV20 showed wound healing promotion on the mouse wound model. Different gradient concentrations of OM-LV20, from 0.5, 1, 2.5, 5, and 10 nM, was respectively applied to the full-thickness skin wound on mice, twice, daily, and it was not observed that OM-LV20 promoted skin wound healing strongly at the concentrations range. However, 20 nM of OM-LV20 strongly promoted skin wound healing on mice, which may be caused by the difference between cells in vitro and animals in vivo. Compared with the negative control, topical skin application of OM-LV20 on full-thickness skin wounds in mice significantly accelerated the repair rate (Figure 6). Furthermore, compared with the application of EGF at the same molar concentration, OM-LV20 also showed a similar acceleration of wound healing in vivo. Some growth factors, that is EGF, have been clinically used to promote wound healing of various tissues. However, compared with small molecule bioactive peptides, growth factors would show higher cost for production, transportation, and storage; and it would be more prudently considered that growth factors may exhibit the "tumor promotion" like effects, which strongly limits their clinical usage. The current small peptide, OM-LV20, containing only 20 amino acid residues might be a potential biocandidate for development of novel wound healing-promoting agent.

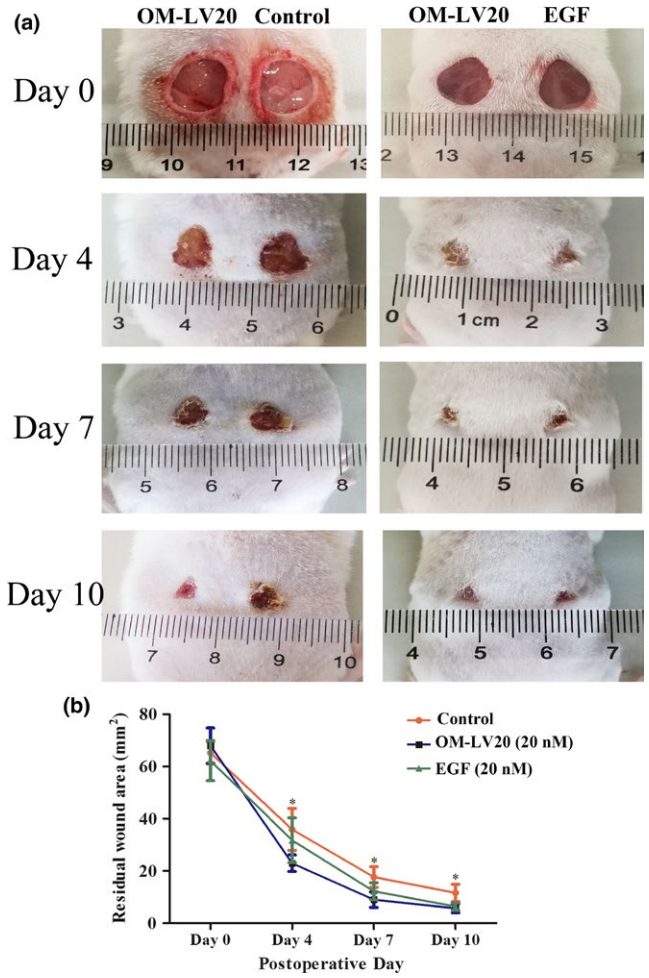


**FIGURE 6** Increase in healing of full-thickness skin wounds in mice following topical application of OM-LV20. Two circular and matching full-thickness skin wounds were made on the backs of mice. The mice were then randomly divided into two groups (10 mice each), with the first group treated with 20 μl of OM-LV20 (20 nM) or saline (indicated as "Control") and the second group treated with 20 μl of OM-LV20 (20 nM) or 20 μl of EGF (20 nM) solution. (a) Images of representative mice were taken on postoperative days 0, 4, 7, and 10. (b) Wound closure was assessed by morphometrical analysis of wound areas (IMAGE J, NIH). Wound residual area was determined ($n = 10$) from three independent experiments. *$p < .05$, **$p < .01$, and ***$p < .0001$ indicate significantly different from the control (Student's $t$ tests)

## 5 | CONCLUSIONS

In this research, a novel peptide was identified from the skin secretions of odorous frog *O. margaretae*. The OM-LV20 peptide sequence was "LVGKLLKGAVGDVCGLLPIC' and contained an intramolecular disulfide bridge located at the C-terminus. OM-LV20 showed no antimicrobial activity, hemolytic activity, or acute toxicity, but did show weak antioxidant activity. Of note, significant wound healing potency of OM-LV20 was demonstrated in vivo and in vitro. Our results provide a novel peptide candidate for the development of wound healing-promoting agents.

## ACKNOWLEDGMENTS

This work was supported by grants from the Chinese National Natural Science Foundation (31660244, 31460571, and 31670776).

## CONFLICT OF INTEREST

All authors declare no potential conflict of interests in this work.

## REFERENCES

[1] M. C. Heng, *Int. J. Dermatol.* **2011**, *50*, 1058.
[2] P. Martin, *Science* **1997**, *276*, 75.
[3] G. S. Schultz, J. M. Davidson, R. S. Kirsner, P. Bornstein, I. M. Herman, *Wound Repair Regen.* **2011**, *19*, 134.
[4] P. Martin, S. J. Leibovich, *Trends Cell Biol.* **2005**, *15*, 599.
[5] C. T. Hess, *Adv. Skin Wound Care* **2011**, *24*, 192.
[6] C. K. Sen, G. M. Gordillo, S. Roy, R. Kirsner, L. Lambert, T. K. Hunt, F. Gottrup, G. C. Gurtner, M. T. Longaker. *Wound Repair Regen.* **2009**, *17*, 763.
[7] J. Hardwicke, D. Schmaljohann, D. Boyce, D. Thomas, *Surg.* **2008**, *6*, 172.
[8] E. G. Karapanagioti, A. N. Assimopoulou, *Curr. Med. Chem.* **2016**, *23*, 3285.
[9] A. A. Kaspar, J. M. Reichert, *Drug Discov. Today* **2013**, *18*, 807.
[10] K. Fosgerau, T. Hoffmann, *Drug Discov. Today* **2015**, *20*, 122.
[11] Y. Wang, Y. Zhang, W. H. Lee, X. Yang, Y. Zhang, *Chem. Biol. Drug Des.* **2016**, *87*, 419.
[12] X. Yang, Y. Wang, Y. Zhang, W. H. Lee, Y. Zhang, *Sci. Rep.* **2016**, *6*, 19866.
[13] D. Barra, M. Simmaco, *Trends Biotechnol.* **1995**, *13*, 205.
[14] J. W. Godwin, N. Rosenthal, *Differentiation* **2014**, *87*, 66.
[15] H. Yokoyama, T. Maruoka, A. Aruga, T. Amano, S. Ohgo, T. Shiroishi, K. Tamura. *J. Invest. Dermatol.* **2011**, *131*, 2477.
[16] M. Suzuki, A. Satoh, H. Ide, K. Tamura, *Dev. Biol.* **2005**, *286*, 361.
[17] M. Mashreghi, M. R. Bazaz, N. M. Shahri, A. Asoodeh, M. Mashreghi, M. B. Rassouli, S. Golmohammadzadeh. *J. Ethnopharmacol.* **2013**, *145*, 793.
[18] M. R. Bazaz, M. Mashreghi, N. M. Shahri, M. Mashreghi, A. Asoodeh, M. B. Rassouli, et al., *Pharm. Biol.* **2013**, *51*, 1600.
[19] M. R. Bazaz, M. Mashreghi, N. M. Shahri, M. Mashreghi, A. Asoodeh, M. B. Rassouli, *Jundishapur J. Microbiol.* **2015**, *8*, e21218.
[20] J. Tang, H. Liu, C. Gao, L. Mu, S. Yang, M. Rong, Z. Zhang, J. Liu, Q. Ding, R. Lai. *PLoS ONE* **2014**, *9*, e92082.
[21] H. Liu, L. Mu, J. Tang, C. Shen, C. Gao, M. Rong, Z. Zhang, J. Liu, X. Wu, H. Yu, R. Lai. *Int. J. Biochem. Cell Biol.* **2014**, *49*, 32.
[22] L. Mu, J. Tang, H. Liu, C. Shen, M. Rong, Z. Zhang, R. Lai. *FASEB J.* **2014**, *28*, 3919.
[23] A. Di Grazia, F. Cappiello, A. Imanishi, A. Mastrofrancesco, M. Picardo, R. Paus, M. L. Mangoni *PLoS ONE* **2015**, *10*, e0128663.
[24] X. Yang, W. H. Lee, Y. Zhang, *J. Proteome Res.* **2012**, *11*, 306.
[25] X. Yang, Y. Wang, W. H. Lee, Y. Zhang, *Toxicon* **2013**, *74*, 151.
[26] K. C. Wen, H. H. Chiu, P. C. Fan, C. W. Chen, S. M. Wu, J. H. Chang, H. M. Chiang *Molecules* **2011**, *16*, 5735.
[27] J. A. Sprowl, G. Ciarimboli, C. S. Lancaster, H. Giovinazzo, A. A. Gibson, G. Du, L. J. Janke, G. Cavaletti, A. F. Shields, A. Sparreboom. *Proc. Natl Acad. Sci.* **2013**, *110*, 11199.
[28] X. Xu, R. Lai, *Chem. Rev.* **2015**, *115*, 1760.
[29] Y. Zhang, *Zool. Res.* **2015**, *36*, 183.
[30] L. Qiao, W. Yang, J. Fu, Z. Song, *PLoS ONE* **2013**, *8*, e75211.
[31] H. Wang, Z. Yu, Y. Hu, F. Li, L. Liu, H. Zheng, H. Meng, S. Yang, X. Yang, J. Liu. *Peptides* **2012**, *35*, 285.
[32] J. Li, X. Xu, C. Xu, W. Zhou, K. Zhang, H. Yu, Y. Zhang, Y. Zheng, H. H. Rees, R. Lai, D. Yang, J. Wu. *Mol. Cell Proteomics* **2007**, *6*, 882.
[33] J. M. Conlon, *Cell. Mol. Life Sci.* **2011**, *68*, 2303.
[34] Z. Chen, X. Yang, Z. Liu, L. Zeng, W. Lee, Y. Zhang, *Biochimie* **2012**, *94*, 328.
[35] Y. Wang, X. Li, M. Yang, C. Wu, Z. Zou, J. Tang, X. Yang. *J. Pept. Sci.* **2017**, *23*, 384.

**How to cite this article:** Li X, Wang Y, Zou Z, et al. OM-LV20, a novel peptide from odorous frog skin, accelerates wound healing in vitro and in vivo. *Chem Biol Drug Des*. 2017;00:1–11. https://doi.org/10.1111/cbdd.13063